

Guide to the Realization of the ITS-90

1 édition 2018

Partie 3

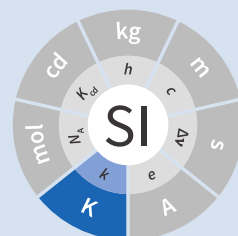
Part 3

Vapour Pressure Scales and Pressure Measurements

Consultative Committee for Thermometry

January 01, 2018

01 janvier 2018



**Guide to the Realization of the ITS-90
Part 3: Vapour Pressure Scales
and Pressure Measurements**

Consultative Committee for Thermometry

1st edition 2018

01 January 2018

Abstract

This paper is a part of guidelines, prepared on behalf of the Consultative Committee for Thermometry, on the methods for how to realize the International Temperature Scale of 1990 (ITS-90).

It discusses the major issues linked to vapour-pressure thermometry for the realization of the International Temperature Scale of 1990 near its lower end.

1. INTRODUCTION

In the temperature range from 0.65K to 5.0K, the ITS-90 is defined using equations relating the vapour pressures of the two helium isotopes ^3He and ^4He to T_{90} (see Equation (3) and Table 3 of the text of ITS-90 [Preston-Thomas 1990]). Between 3.0K and 5.0K, these equations allow to realize the lowest of the three calibration temperatures for a constant-volume gas thermometer used as interpolation instrument in the range from 3.0K to the triple point of neon (24.5561K), see ITS-90 Guide Chapter 4 *Gas Thermometry* [Steur *et al.* 2015]. Furthermore, vapour-pressure-temperature relations for equilibrium hydrogen valid in narrow temperature ranges (16.9K to 17.1K and 20.26K to 20.28K, respectively) are prescribed (see Equations (11a) and (11b) in [Preston-Thomas 1990]). These equations may be used to determine calibration temperatures for standard platinum resistance thermometers, see ITS-90 Guide Chapter 5 *Platinum Resistance Thermometry* [Pokhodun *et al.* 2016]. Best estimates of the deviation of the ITS-90 vapour-pressure temperatures from thermodynamic values are given in an appendix of the *Mise en pratique of the definition of the kelvin (MeP-K)* [CCT 2010, Fellmuth *et al.* 2016, http://www.bipm.org/en/publications/mep_kelvin/].

There are three principal requirements for any vapour-pressure thermometer, namely to know the vapour-pressure-temperature relationship; to arrange for a volume of the pure liquid and vapour phases to come to equilibrium; and to measure absolutely the pressure at the (plane) interface. The main physical effects influencing the determination of vapour pressures are (i) the aerostatic head due to the gas column, (ii) the thermomolecular pressure difference, (iii) the formation of cold spots, and (iv) the possible formation of thermal oscillations.

The techniques by which vapour pressures can be set up and measured are described in this chapter starting with examples for typical vapour-pressure systems. Since the demands concerning the pressure measurement are challenging especially near to the lower limit of 100Pa, cf. Table 1, an overview of this topic is also given for the relevant pressure range. Finally, a representative uncertainty budget is discussed.

The examples for typical vapour-pressure systems presented in this document are only helium vapour-pressure thermometers. The construction principles can also be applied for hydrogen systems. But three special problems in realizing the two hydrogen boiling points have to be considered:

- A catalyst in the liquid chamber is necessary to ensure that the hydrogen has the equilibrium composition of the two nuclear-spin isomers (often designated by the prefixes *ortho* and *para*). The materials most commonly employed for this purpose have been transition metal oxides and rare-earth oxides, see the detailed discussion in [Fellmuth *et al.* 2005]. The use of a catalyst is of course dangerous with respect to not introducing sources of impurities. Furthermore, it has to be considered that all catalysts for *ortho-para* conversion are chemically active substances and an activation of catalytic effectiveness may be necessary.
- The vapour-pressure temperature may depend on whether gas has been removed from or added to the sample chamber because of isotopic composition effects. Isotope fractionation may result in a temperature difference of 0.4mK between the dew point (vanishingly small liquid fraction) and the boiling point (vanishingly small vapour fraction). In practice, the boiling point is used since the catalytic action is more efficient if the free liquid is in contact with the catalyst.
- The influence of the isotopic composition is very large for hydrogen, see the Technical Annex of the *MeP-K*. The Technical Annex is mandatory for the realization of the ITS-90

and specifies the isotopic composition of hydrogen. This specification is not included in the scale definition itself.

Table 1. Pressure and pressure sensitivity of some helium and hydrogen vapour-pressure points that are used as defining fixed points.

Substance	Temperature T_{90}/K	Pressure p/Pa	Absolute Sensitivity $dp/dT_{90}/(\text{Pa} \cdot \text{K}^{-1})$	Relative Sensitivity $d \ln p/dT_{90}/(1/\text{K})$
^3He	0.65	115.91	1081	9.325
	1.0	1160.11	5501	4.741
	1.5	6709.28	17 797	2.653
	2.0	19 999.2	36 348	1.817
	2.5	44 018.4	60 715	1.379
	3.0	81 825.7	91 831	1.122
	3.1968	101 321	106 572	1.052
	3.2	101 662	106 826	1.051
	1.25	114.73	757	6.598
	1.5	471.54	2289	4.854
^4He	2.0	3129.7	9200	2.939
	2.1768	5041.8	12 408	2.461
	2.5	10 227.8	20 062	1.962
	3.0	24 046.4	36 018	1.498
	3.5	47 045.4	56 773	1.207
	4.0	81 616.2	82 330	1.009
	4.2221	101 325	95 330	0.941
	4.5	130 260	113 235	0.869
	5.0	196 016	151 189	0.771
	17.035	33 321.3	13 320	0.400
H_2	20.27	101 292	30 000	0.296

2. VAPOUR-PRESSURE RELATIONS

2.1. Helium vapour-pressure relations

The vapour-pressure relations for helium are of the form

$$T_{90}/\text{K} = A_0 + \sum_{i=1}^9 A_i [\ln(p/\text{Pa}) - B/C]^i. \quad (1)$$

Values of the constants A_0 , A_i , B and C are given in Table 3 of the Text of the ITS-90 for the three ranges 0.65K to 3.2K for ^3He ; 1.25K to 2.1768K for ^4He ($^4\text{He II}$); and 2.1768K to 5.0K also for ^4He ($^4\text{He I}$)⁽¹⁾. The ^4He equations coincide at the lambda point (2.1768K, 5041.8Pa) with a first derivative $\text{d} \ln p / \text{d} T_{90}$ of 2.461K^{-1} . In deriving these equations, no constraints were placed at the second derivative, which is discontinuous at this point.

The upper temperature limits for the use of the two helium isotopes were chosen to be somewhat below the critical points, since the specification of the relationship and measurement of vapour pressures become matter of some difficulty as the critical point is approached. The lower temperature limit was caused by the fact that when the ITS-90 was established, it did not appear possible to measure widely pressures below 100Pa with a relative uncertainty sufficient for reaching the desired temperature uncertainty of order 0.1mK, cf. Table 1 and Figure 1.

⁽¹⁾ In the phase diagram of ^4He , the liquid phases above and below the lambda line are distinguished by referring them as $^4\text{He I}$ and $^4\text{He II}$, respectively. The properties of superfluid $^4\text{He II}$ are very different from those of $^4\text{He I}$.

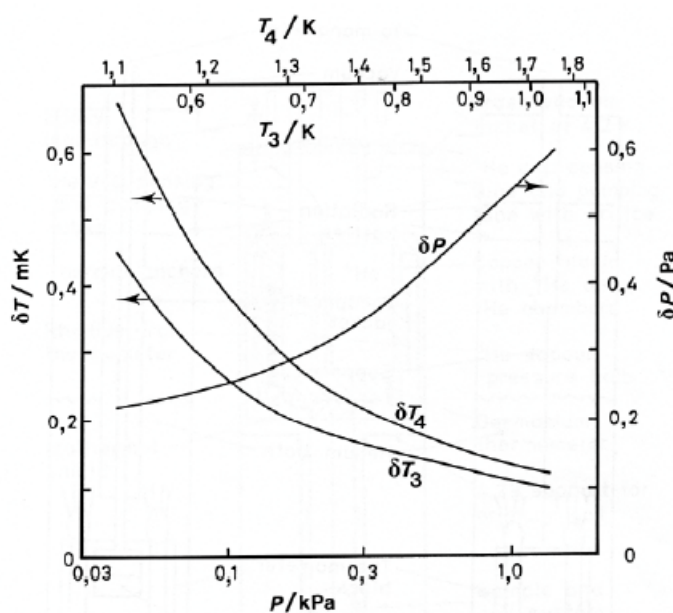


Figure 1 — Examples of uncertainties in pressure measurements using a capacitance diaphragm pressure gauge below 1.3kPa, and the equivalent uncertainties δT_3 and δT_4 in temperatures T_3 and T_4 for ^3He and ^4He vapour-pressure measurements, respectively [Rusby and Swenson 1980]. © Bureau International des Poids et Mesures. Reproduced by permission of IOP Publishing. All rights reserved.

The equations adopted in the ITS-90 are a restricted set of those derived by Rusby and Durieux (1984), which themselves were simplified forms of the equations of Durieux and Rusby

(1983) that were approved by the CIPM (1982) following the introduction of the International Temperature Scale EPT-76 [Durieux *et al.* 1979], see ITS-90 Guide Chapter 1 *Introduction*. The unrestricted forms are useful for those choosing to use them at temperatures close to the critical points or below 0.65K.

2.2. Hydrogen vapour-pressure relations

For the calibration of standard platinum resistance thermometers, see ITS-90 Guide Chapter 5 *Platinum Resistance Thermometry*, two calibration temperatures may be determined by boiling points of equilibrium hydrogen, see Subsection 1. The two temperatures must lie within the ranges 16.9K to 17.1K and 20.26K to 20.28K, respectively. The precise values have to be determined by the following vapour-pressure-temperature relations:

$$T_{90}/\text{K} - 17.035 = (p/\text{kPa} - 33.3213)/13.32, \quad (2)$$

$$T_{90}/\text{K} - 20.27 = (p/\text{kPa} - 101.292)/30. \quad (3)$$

Equation (2) is valid for the range 16.9K to 17.1K, and Equation (3) for 20.26K to 20.28K.

3. VAPOUR-PRESSURE SYSTEMS

3.1. Systems immersed in liquid baths

In its simplest form, a ^4He vapour-pressure thermometer consists of a vessel containing the liquid in equilibrium with its vapour, and the thermometer liquid is also the refrigerating liquid. This is possible because ^4He can be transported in transport vessels and all impurities freeze out. (The only relevant impurity ^3He has a negligible natural abundance.) A schematic illustration of a cryostat for calibrating capsule-type thermometers is given in Figure 2a. The vapour pressure is sensed via a tube inserted into the vapour space and terminating above the liquid surface. The pressure is usually regulated by means of a throttling valve in the pumping line (not shown). The pressure, and hence the temperature, is progressively reduced so as to prevent large temperature stratification. An electrical heater at the bottom of the liquid (not shown) can be used for reheating and, at low power levels, will promote mixing.

Below the lambda point, the phenomenal thermal diffusivity of ^4He II ensures that under stable conditions no temperature gradients exist within the liquid. In this case the system of Figure 2a can be used for high-accuracy vapour-pressure measurements. The only limitations are the ability of the pump to reduce the temperature as far as required and, possibly, the appearance of thermomolecular effects at low pressures. The latter limitation is eliminated by use of a tube of inner diameter 10mm or more equipped with appropriate radiation baffles. Above the lambda point, the convection mechanism in ^4He I is a feeble one at these temperatures, and significant temperature gradients can be present in the liquid. Such gradients occur even when the temperature monotonically decreases with time. Their magnitude being likely to increase as the temperature is lowered. At 4.2K, the hydrostatic head (pressure increase due to the liquid column) causes a gradient of $12\mu\text{K} \cdot \text{mm}^{-1}$. Temperature differences perhaps become as high as 5mK at the lambda point [Cataland *et al.* 1962]. On reheating, the temperature of the bulk liquid may respond only slowly if the pressure is allowed to rise, and gross gradients can then result.

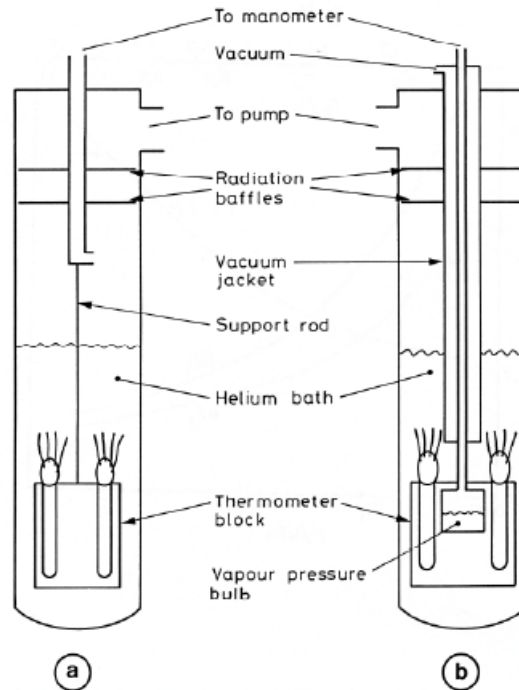


Figure 2 — Schematic illustrations of systems for realizing ^4He vapour pressures: using a bath of liquid (a), suitable for $^4\text{He II}$, and a bulb (b) for $^4\text{He I}$, unsuitable for $^4\text{He II}$. Thermal shields around the helium bath are not shown.

The difficulties with temperature gradients in the thermometer liquid $^4\text{He I}$ can be avoided by mounting the thermometers in a copper block containing a vapour-pressure bulb (Figure 2b) that is independently supplied with helium, so that a liquid-vapour interface is contained within it. In a closed system, the liquid fraction will increase when the temperature is reduced, and the total amount of helium must be such that the bulb does not overfill. The supply tube (of stainless steel or another material of low thermal conductivity, and typically 2mm inner diameter) is also the pressure-sensing tube. Where it passes through the surrounding liquid, it must be insulated sufficiently well to avoid condensation within it (cold spots). Light insulation is reported as being sufficient for this purpose, since cold spots tend to be self-stifling by virtue of the heat of condensation [Ambler and Hudson 1956]. However, a stainless-steel vacuum jacket is often used and may extend up to room temperature. In addition, copper cladding or electrical heaters on the sensing tube can be used. These have the advantage of keeping the sensing tube and vapour within it relatively warm, only reaching the liquid temperature just above the bulb, thereby reducing the aerostatic-head correction. For an exposed tube and a bulb at 4.2K, this correction may be about 0.5mK, compared with 0.1mK to 0.2mK that is typical for a vacuum-jacketed tube. For the latter one, however, the temperature distribution, needed for calculating the pressure head, can be difficult to ascertain. At the lower temperatures, aerostatic-head corrections are smaller in terms both of pressure and of the temperature equivalents, because of the rapid decrease of vapour density with decrease in temperature.

No radiation trap is shown inside the pressure sensing tube of Figure 2b. If this is 2mm in diameter, radiative heat transfer down the tube (assuming that all the radiation emitted at room temperature is adsorbed in the bulb) would be about 1.4mW. The helium in the bulb is not likely to absorb much of this, while the copper block could easily do so without setting up

significant temperature gradients. A trap could be included near the bottom of the tube, but it would need careful design. A simple bend in the tube is unlikely to be effective, while any other system must be so constructed that no liquid can be held at that point. Even with a straight tube, it is possible for liquid to block the tube just above the bulb, leading to substantial measurement errors. A pressure pulse may dislodge such a block, but as a matter of design, the portion of the tube exposed to low temperatures should be short, or the vacuum jacket can be extended right down to the bulb. In the latter case, the heat conducted down the sensing tube, perhaps 0.1mW, can be readily absorbed in the block. But a baffle must be included in the vacuum jacket to intercept the radiation from room temperature components of the jacket. There will be some differential contraction between the sensing tube and the vacuum jacket. These must not touch, and an insulating spacer, which can also serve as the radiation trap, should be used to prevent this. Alternatively, bellows or a sliding seal at the upper end of the tube can prevent touching.

While a vapour-pressure bulb contained in a copper block is preferable for normal helium, ^4He I, this is not the case for superfluid ^4He II. With ^4He II in the bulb, a superfluid film would creep up the walls of the sensing tube, would evaporate at some higher temperature, and would then reflux back to the bulb. This action can result in a measurement error of several millikelvins [Sydoriak *et al.* 1964] due in part to pressure gradients in the tube and in part to temperature gradients in the bulb. In vacuum-isolated systems, an orifice in the lid of the helium bulb can reduce the film flow, see Section 3.2. Continuity of measurements on passing through the lambda point is a good test of any design. By contrast, the system of Figure 2a works well below the lambda point. In this system, the superfluid film evaporates as part of the cooling process and never affects the pressure sensing. Clearly a dual system, in which both a vapour-pressure bulb and a bath pressure-sensing tube are provided, would enable the complete ^4He range to be covered, and would also allow investigations of the differences between the two realizations to be made.

3.2. Vacuum-isolated systems

Most of the realizations of helium vapour-pressure scales were performed applying systems, in which copper thermometer blocks containing vapour-pressure bulbs were suspended inside a vacuum jacket [Sydoriak *et al.* 1964, El Samahy 1979, Rusby and Swenson 1980, Meyer and Reilly 1996, de Groot *et al.* 1993 and 1997, Hill 2002, Engert and Fellmuth 2003, Engert *et al.* 2007, Shimazaki *et al.* 2011, Sparasci *et al.* 2011b]. Sydoriak *et al.* (1964) have performed extensive comparisons of the vapour pressures of ^3He and ^4He prior to the derivation of the 1962 ^3He vapour-pressure scale and equation, cf. [Quinn 1990]. These comparisons were performed in an apparatus designed to reduce the number and magnitude of corrections associated with the refluxing film in the ^4He pressure-sensing tube and the attached bulb. Problems with ^3He are its high cost and the need to take into account of contamination with ^4He . Because of its cost, ^3He is usually kept in a closed system and repeatedly used. As typical examples, the vapour-pressure systems of Rusby and Swenson (1980) and Engert *et al.* (2003, see p. 24) and (2007, see p. 24), respectively, are described in detail in the following. In both cases, the vacuum jacket is immersed in a liquid ^4He bath. Nowadays preferably cryostats designed around closed-cycle cryocoolers are applied for high-accuracy low-temperature thermometry. Examples of modern systems are given in [Steele 1997, Hill and Steele 2003, Sakurai 2003, Nakano *et al.* 2007, Pavese *et al.* 2011, Sparasci *et al.* 2011a, Yang *et al.* 2011, Shimazaki *et al.* 2011, Pavese and Molinar Min Beciet 2013]. These cryostats allow measurements to be performed for extremely long periods (months), uninterrupted by

disturbances usually caused by refilling liquid refrigerant. Up to now, vapour-pressure systems without ^4He baths are not realised. In realising such system, the main design principles for the vapour-pressure part discussed below have to be considered.

A combined ^3He and ^4He vapour-pressure cryostat, somewhat simpler than that of Sydoriak *et al.* (1964), has been described by Rusby and Swenson (1980) and was used by them for the re-determination of the vapour-pressure relations, see Figure 3. The copper thermometer block containing the helium bulbs was suspended inside a vacuum jacket, which was surrounded by liquid ^4He at 4.2K. A single 50cm³ bulb of ^4He was used for cooling and sensing the vapour pressure. The problem of film flow was avoided by including an orifice of 0.6mm diameter in the lid of the bulb. Such film as flowed through the orifice was soon evaporated and thereby contributed to cooling. The pressure-sensing tube joined the 6mm diameter pumping tube some 40mm higher up and so was not affected by film refluxing. The pressure drop across the orifice and along this section of the tube was negligible at temperatures above 1.4K. A larger orifice could have permitted accurate measurements to still lower temperatures. The ^4He bulb contained a spiral of copper foil to promote temperature uniformity (see the authors' discussion of measurements above and below the lambda point).

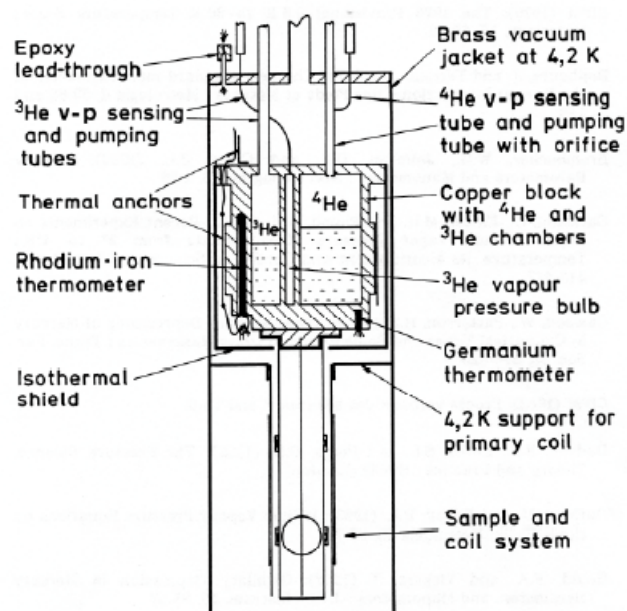


Figure 3 — A schematic diagram of the cryostat used by Rusby and Swenson [1980] for CMN magnetic thermometry and for ^3He , ^4He I and ^4He II vapour-pressure measurements. © Bureau International des Poids et Mesures. Reproduced by permission of IOP Publishing. All rights reserved.

A ^3He cooling chamber was provided, and measurements of ^3He vapour pressures were made with a small 1cm³ bulb (5mm diameter by 60mm long) and a sample of purified gas. The vapour-pressure tubes were 2mm in diameter at temperatures up to 4.2K, and 6mm (for ^4He) and 5mm (for ^3He) above this. These dimensions give thermomolecular effects, calculated from the Weber-Schmidt equation (see Section 4.2, see p. 20), equivalent to 1mK at 1.25K and 0.65K for ^4He and ^3He , respectively, with the effects increasing rapidly at lower temperatures. If tubes with larger diameters are used at higher temperatures, the temperature of the junctions must, of course, be known, but this is desirable in any case for the calculation of the aerostatic head effect. The vapour-pressure sensing tubes used by Rusby and Swenson

passed through the ^4He bath and the aerostatic head was consequently quite large (equivalent to values as large as 0.6mK). Small lengths of yarn were inserted into the tubing at room temperature to reduce thermal oscillation effects. An alternative could be to enlarge the tubes. Cold spots were not evident in measurements at 4.2K, but measurements of pressures above atmospheric were made only when the liquid level in the main helium bath had fallen below the top of the vacuum jacket, and with the bath pressurised to a maximum of 0.2MPa (absolute). In this or any similar system, the tubing that is at room temperature but is open to the cryogenic area must be clean, as any desorbed gases will diffuse into the cryostat and be re-adsorbed there. The pressure gradient due to this diffusion can be significant at low pressures.

A special design of a ^3He vapour-pressure thermometer was used by Engert *et al.* (2003, see p. 24) and (2007, see p. 24) to reduce drastically the uncertainty of the corrections associated with the aerostatic head and the thermomolecular pressure difference. The principal design of the different pressure-sensing tubes is shown in Figure 4. The upper parts, extending from room temperature down to the inner vacuum can (IVC) flange, are made of stainless steel. Below the 80K level, they are vacuum isolated. The temperatures of the tubes at the IVC flange level can be varied from 4.2K to 30K. Inside the IVC, i.e. from the IVC flange level to the vapour-pressure bulb located in the experimental platform, two vertical copper tubes are connected with three horizontal stainless steel tubes. The temperatures of the copper tubes can be stabilised in the range from 0.6K to 20K using heaters and thermal links to the 1K pot and the mixing chamber (MC) of the dilution refrigerator, respectively. The temperature differences between the main stainless-steel tube above the IVC flange level, the copper tubes, and the bulb are concentrated on the interconnecting horizontal tubes. These tubes have a small angle of inclination to avoid condensation of liquid in parts other than the bulb. The inner diameters of the largest pressure-sensing tube are as follows, with the typical temperature distribution in parentheses: 35mm (300K to 80K), 17mm (80K to 8K), 5.4mm (8K to 2.2K), 4mm (2.2K), 2mm (2.2K to 1.4K), 3mm (1.4K), 2mm (1.4K to the temperature of the bulb). For this tube, the temperature equivalent of the thermo-molecular pressure difference has been estimated to be smaller than 0.03mK at 0.65K applying the approximated Weber-Schmidt equation (see Section 4.2, see p. 20). The temperature equivalent of the overall aerostatic-head correction at 10kPa, i.e. at 1.7K, is of order of 0.5mK with a standard uncertainty of 0.015mK. The temperature stabilisation of the tubes at specified levels prevented thermal oscillations caused by condensation and evaporation of liquid as well as the formation of cold spots.

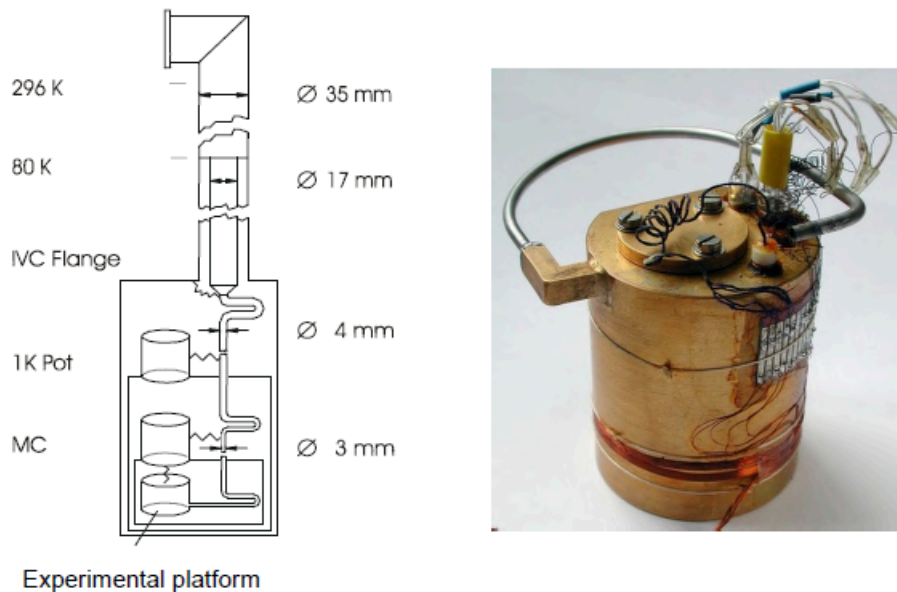


Figure 4 — ^3He vapour-pressure thermometer built at the Physikalisch-Technische Bundesanstalt (PTB) [Engert *et al.* 2003 and 2007]: On the left: Schematic sketch showing the principal design of the pressure-sensing tubes (IVC inner vacuum can, MC mixing chamber of the dilution refrigerator). The thermal links are indicated by the zigzag lines. On the right: Photograph of a vapour-pressure bulb with a horizontal stainless-steel part of the pressure-sensing tube and different capsule-type rhodium-iron resistance thermometers installed. Figure reproduced with the permission of AIP Publishing.

Three quite different vapour-pressure bulbs were used, the volume-to-surface ratios of which vary by an order of magnitude. A significant influence of this ratio could be ruled out. At the bottom of each of the vapour-pressure bulbs, a layer of pressed copper ($< 60\mu\text{m}$) or silver (70nm) powder ensures good thermal contact between the liquid helium and the body of the bulb. For all bulbs, the effect of the filling level with liquid ^3He as well as the effect of different high-purity ^3He samples (99.9999 atom % nominal purity) on the determination of the vapour pressures was estimated to be of the order of about 0.01mK temperature equivalent. Because the cryogenic set-up allowed the variation of the temperature distribution along the pressure-sensing tubes, it was possible to check the influence of heat input from the tubes into the bulbs. The temperature of the individual low-temperature parts of the tubes was changed stepwise for each vapour pressure measured. The extrapolation to zero of the dependence of the bulb temperature on the temperature difference between the bulb and the lowest vertical part of the tube enabled the determination of vapour-pressure values for zero heat input. Furthermore, this made the data highly repeatable. Applying the optimised vapour-pressure bulb shown in Figure 4, a repeatability of a few 0.01mK temperature equivalent was obtained for the results of an individual run. The repeatability of the ^3He vapour-pressure realizations for all nine runs performed was about 0.12mK standard deviation. This value includes the influence of all different designs of the bulbs and tubes. In the last four runs using the same optimised set-up, the repeatability was of order of 0.03mK . For the temperature range from 0.65K to 1K , the complete uncertainty budget for the calibration of rhodium-iron resistance thermometers against the ^3He vapour-pressure scale is given in Table 2. The pressure measurement was

performed applying capacitive diaphragm gauges (CDGs), which were calibrated from 50Pa to 1.3kPa against the vacuum primary static-expansion standard of the PTB.

Table 2. **Uncertainty budget for the calibration of rhodium-iron resistance thermometers against the ^3He vapour-pressure scale at PTB [Engert *et al.* 2007] (CDGs capacitive diaphragm gauges, EP experimental platform). ΔT stands for temperature difference. Uncertainty values are in mK.**

Source of uncertainty	T_{90}/K				
	0.65	0.75	0.85	0.95	1
Resistance bridge	0.020	0.020	0.020	0.020	0.020
Standard resistor	0.003	0.003	0.003	0.003	0.003
Correction of resistance to zero current	0.020	0.020	0.020	0.020	0.020
Calibration of the CDGs	0.087	0.109	0.133	0.158	0.171
Repeatability of the CDGs	0.021	0.027	0.033	0.039	0.042
Fit to the calibration data of the CDGs	0.017	0.022	0.026	0.031	0.034
Enclosure temperature of the CDGs	0.005	0.007	0.008	0.010	0.011
Offset drift of the CDGs	0.005	0.005	0.004	0.002	0.001
Head correction	0.015	0.015	0.015	0.015	0.015
Thermo-molecular pressure difference	0.003	0.001	0.000	0.000	0.000
Extrapolation to zero heat input into the bulb	0.040	0.040	0.040	0.040	0.046
Volume-to-surface ratio of the bulb	0.010	0.010	0.010	0.010	0.010
Filling level of the bulb with liquid	0.010	0.010	0.010	0.010	0.010
Purity of ^3He gas sample	0.010	0.010	0.010	0.010	0.010
ΔT between the EP and the thermometers	0.010	0.010	0.010	0.010	0.010
ΔT between the EP and the bulb	0.010	0.010	0.010	0.010	0.010
ΔT in the EP	0.020	0.020	0.020	0.020	0.020
Drift correction	0.020	0.020	0.020	0.020	0.020
Repeatability of calibration measurements	0.120	0.120	0.120	0.120	0.120
Combined standard uncertainty	0.163	0.178	0.195	0.214	0.226

4. PRESSURE MEASUREMENTS

4.1. Primary standards and transducers for pressure measurements

Pressure measurements are required for the realization of the helium vapour-pressure scales, the boiling points of hydrogen and the interpolating gas thermometer, see ITS-90 Guide Chapter 4 *Gas Thermometry*. Table 1 summarises helium and hydrogen vapour-pressure data and allows the measurement requirements to be calculated. It shows that in order to cover the complete range for ^4He , it is necessary to measure absolute pressures from 100Pa to 200kPa, with standard uncertainties of 0.1Pa to 15Pa (relative 0.1% to 75ppm, ppm means parts per million), respectively, to achieve 0.1mK uncertainty in T_{90} . The needed relative uncertainties are less wide ranging, varying from 30ppm for hydrogen at 20.3K to 0.1% for ^3He at 0.65K. For gas thermometry, the range is 30ppm at 3K to 4ppm at 25K. A measuring instrument with a constant relative uncertainty is thus more suitable than one with a constant absolute uncertainty.

Compared with the high-level realizations of the pressure scale, the requirements (in terms of room temperature capability for pressure measurement) of vapour-pressure thermometry are not overly stringent. In the pressure range of interest here, the primary pressure standards of the national metrological institutes are based on liquid-column manometers and pressure balances. Their typical relative uncertainties range from 100ppm at 100Pa to a few ppm at 200kPa [Miiller *et al.* 2002, Pavese and Molinar Min Beciet 2013]. The smallest relative uncertainty achieved with pressure balances above 70kPa amounts to 0.7ppm [Zandt *et al.* 2015].

An overview of transfer standards for absolute pressure measurements is given in Chapter 8 of the book *Modern Gas-Based Temperature and Pressure Measurements* [Pavese and Molinar Min Beciet 2013]. From the standpoint of the various operating principles, they are grouped as follows: Piezoresistive transducers, optical transducers, force-balance transducers, capacitance transducers, and vibrating-structure transducers. Criteria for the selection of an appropriate pressure measuring device are the pressure range, the uncertainty, the resolution, the dependence of the signal on temperature, linearity and hysteresis. Considering these criteria, the application of the two primary pressure standards, namely liquid-column manometers and pressure balances, see below, can be recommended for vapour-pressure thermometry. As transfer standards, non-rotating (force-balanced) pressure balances and capacitive diaphragm gauges (CDGs) are suitable. On the contrary, quartz-Bourdon tube transducers should not be used because the diffusion of helium into the quartz tube causes large drifts.

A well-defined calibration method should be applied to make sure that a transducer is good enough to be used as a transfer standard at the desired uncertainty level. For checking the metrological characteristics of the transducer, the stability of the transducer output signal at zero pressure should be carefully determined for a long time. Calibration shifts are frequently dominated by the zero signal shift. The calibration should be carried out with repetitive tests for both increasing and decreasing pressures, made at different times. Full-scale pressure drift should also be determined in order to understand whether some fatigue or creep effects may influence the readings.

4.1.1. Liquid-column manometers

Liquid-column manometers are mostly mercury manometers. They are generally limited to 120 kPa. The classical method employs a cathetometer to determine the position of the mercury levels in a U-tube manometer, and has a limit of uncertainty of about 3 Pa. Smaller uncertainties can be attained if the levels are sensed by capacitive techniques or interferometric techniques (white-light, laser or ultrasonic interferometry) [Tilford 1993/1994 and the references therein, Alasia *et al.* 1999a and 1999b, Sadkovskaja and Eichwald 2011, Pavese and Molinar Min Beciet 2013]. For pressures of the order 100 kPa, such instruments can measure absolute pressures with a relative uncertainty of about a few ppm, and pressure ratios of about 1 ppm.

At these levels of accuracy, uncertainties in length, density of mercury, which is pressure and temperature dependent, aerostatic head, mercury vapour pressure and capillary depression may become critical. For absolute pressure measurements, the knowledge of the local value of the acceleration due to gravity is required. A sufficiently accurate value of gravity may be obtained by using the *Réseau Gravimétrique Unifié 1971 (IGSN-71) de l'Union Géodésique et Géophysique Internationale*.

In the paper of Sommer and Poziemski (1993/1994), all literature data of high-accuracy determinations of mercury density are compared. The overall set of measurements at 20°C differs by 3 ppm from one another, exceeding the typical stated uncertainty of 1 ppm. An analysis is also given concerning the thermal expansion and compressibility coefficients. Functions are given both for the dependence of the density on temperature and pressure.

Corrections for the errors mentioned above are straightforward, except the capillary depression of mercury surfaces of less than several centimetres in diameter, which remains a potential source of uncertainty in high-precision manometry [Brombacher *et al.* 1960]. Tables for the capillary correction in terms of bore diameter and meniscus are given in [Kistemaker 1944-46, Cawood and Patterson 1933]. Gould and Vickers (1952) computed similar tables for values of the coefficient of surface tension ranging from 0.4 nm^{-1} to 0.5 nm^{-1} . Within this range, for a given meniscus height, the capillary depression is practically linearly dependent on the coefficient of surface tension. In practice, this coefficient appears to vary from 0.4 nm^{-1} to 0.58 nm^{-1} depending on the degree of surface cleanliness of the mercury and the surface conditions of the container. There is frequently a degree of hysteresis in the relation between meniscus height and pressure. The lack of a precise knowledge of the coefficient of surface tension is such that if an uncertainty within 10 Pa is desired, a tube of diameter not less than 15 mm should be used. To achieve the highest levels of accuracy, the diameter of the mercury surface should be so large ($\geq 30 \text{ mm}$) that the uncertainty in the capillary depression will be acceptable ($\leq 0.15 \text{ Pa}$).

4.1.2. Pressure balances

For this instrument, the pressure is defined by the local value of gravity, the mass and the effective area of a piston freely rotating in a closely-fitting cylinder. Pressure settings for a given piston are changed by changing the mass, i.e. by adding additional weights. The following review books and survey papers deal with the application of pressure balances: Dadson *et al.* (1982), Sutton and Fitzgerald (2009), Pavese and Molinar Min Beciet (2013). Limited by the mass of the rotating piston, pressures down to a few kPa can be measured.

The principal limitation is the accuracy with which the effective area is known. This may be obtained from direct dimensional measurement (primary realization of pressure standards) [Sabuga 2011a, Zandt *et al.* 2015] or, more usually, from calibration against

another pressure balance, or against a mercury manometer near standard atmospheric pressure, where this device too has high relative accuracy, see above. For stainless steel the temperature and pressure coefficients of the effective area amount to (order of magnitude) $2 \times 10^{-5} \text{K}^{-1}$ and $-5 \times 10^{-6} \text{MPa}^{-1}$, respectively, and for tungsten carbide to $1 \times 10^{-5} \text{K}^{-1}$ and $-3 \times 10^{-6} \text{MPa}^{-1}$. Some approximate means of measuring the temperature of the piston-cylinder assembly should be, therefore, included. The calibration of the weights should not be a problem, even allowing for the need for buoyancy corrections if the weighing is performed in air. For pressure measurements in absolute mode, where around the weights a stable appropriate vacuum reference pressure is generated, measured and corrected for, no buoyancy corrections are necessary. The gas head may vary by about 2cm as the piston sinks in use, which for helium is equivalent to only a few parts in 10^7 at standard atmospheric pressure.

Pressure balances are not so much gauges of pressure as generators of a series of pressures, whose values are determined by the fixed effective area and the variable loading. Since a continuum of pressures is not available, and because the assembly will need to be taken apart for occasional cleaning, it is usual to apply the generated pressure to the reference port of a differential CDG. The vapour pressure to be measured is fed to the other port and the CDG output gives the difference between the two. In general, the CDG needs to be calibrated, see Section 4.1.4. But for measurements of vapour pressure, the calibration can be avoided by so adjusting the liquid temperature that the CDG reads zero, i.e. that the pressure to be measured exactly equals the pressure generated by the balance. The true zero of the CDG can be simply checked by cross connecting the two sides of the CDG.

For measurements of ^4He vapour pressures, it is convenient to operate the balance with helium, drawing gas from the vapour-pressure system as needed. For ^3He , however, the cost of the gas usually precludes this, while ^4He should not be used for fear of contaminating the ^3He . Air, nitrogen or argon will be convenient, but once ^3He is admitted to the DCG care must be taken not to allow air into the ^3He line. Cross connection to check zero entails some wastage of gas and for ^3He should preferably be carried out only immediately before and after a series of measurements, the minimum requirement.

As was mentioned earlier, the lower limit of operation of the pressure balance is that which supports just the unloaded floating member, which may be the piston or the cylinder, according to design. This can be reduced by choosing a light assembly with a large effective area, and a typical minimum pressure is 2kPa. The pressure balance can achieve a relative uncertainty within about 10ppm (minimum of order 1ppm [Zandt *et al.* 2015]) and a resolution of 1ppm at pressures around 100kPa and above. The relative uncertainty is dominated by that of the effective area, which is usually independent of the pressure above about 10kPa. At lower pressures, it may increase due to a change of the gas flow in the clearance between piston and cylinder, see the overview of experimental literature data given in [Priruenrom 2011] and the theoretical treatment in [Sabuga *et al.* 2011b]. The absolute resolution of a pressure balance has usually an order of 0.1Pa.

4.1.3. Non-rotating (force-balanced) pressure balances

For pressures below the lower limit of the classical pressure balances with rotating piston or cylinder (traditional “floating” piston gauges) treated above, non-rotating pressure balances with large effective areas have been developed. An original device was, for example, described by Ooiwa (1989, see p. 25) and (1993/1994, see p. 25). An overview of the development and the design of two commercial devices is given in [Pavese and Molinar Min

Beciet 2013]. The two devices are the Force Balanced Piston Gauge (FPG) and the Furness Rosenberg Standard (FRS).

DH Instruments [Delajoud and Girard 2002, Haines and Bair 2002] developed the idea of FPG in order to cover the gauge and absolute pressure range from 1Pa to 15kPa. The difference in pressure acting on the effective area of the piston generates a change in force measured by a mass comparator. The non-rotating piston (material tungsten carbide, nominal effective area 9.8cm²) is attached at its center of gravity to the force balance by a linkage. It is stabilised by a small lubrication gas flow from the middle of the cylinder where clearance is larger. An automated pressure controller is used to adjust the flow across the different restrictions and to set and control pressure stability. With this system, which requires clean environment and full knowledge of the controlling part of the instrument, it is possible to have a pressure resolution of order 1mPa and a measurement uncertainty as low as $5\text{mPa} + 3 \times 10^{-5}p$, with p expressed in pascal. The FPGs are now very diffused in national metrology institutes, and different studies have been made [Otal and Legras 2005, Haines and Bair 2009, Hendricks and Olsen 2009] that support the order of magnitude of the claimed uncertainty. For vapour-pressure thermometry, an isolating CDG, see below, should be used to prevent humidified gas coming from FPG entering the system.

The working principle of the FRS is described in [Rendle 1993/1994, Rendle and Rosenberg 1999]. The main part is the piston-cylinder assembly, where the centring of the piston is ensured with flexible hinges designed as a parallelogram suspension system. The pressure on the working side is set by means of an external flow controller plus three manually operated dosing valves. The force on the piston area is detected by a balance with an electromagnetic force compensation working principle integrated on the reference side. The electronic balance mechanism is held at zero when only the piston is balanced. Bock *et al.* (2009) have characterised a system with an effective area of the piston of about 45cm² in the absolute mode. Its resolution was 2mPa and the full range 11kPa. The measured relative standard uncertainty ranges from 7×10^{-4} at 30Pa to 3×10^{-5} at 1kPa. The relative uncertainty of 2×10^{-4} at 100Pa corresponds to a temperature equivalent of 0.02mK for measuring the vapour pressure of ³He at 0.65K, see Table 1.

4.1.4. Capacitance diaphragm gauges

A capacitance diaphragm gauge (CDG) consists of a thin, often metal, membrane under tension located between two electrodes, see for instance [Sullivan 1985]. Deflection of the membrane caused by a pressure difference across it can be accurately detected by capacitance-bridge techniques. CDGs are available with 100Pa to 1MPa ranges. High accuracies require precise temperature control and isolation from vibrations. Even for absolute measurements, differential CDGs are recommended because the vacuum at the reference side can be checked, and if necessary improved. Any mechanical stress to the diaphragm should be avoided that could be caused, for instance, by removing or attaching sealing close to the CDG head. Furthermore, an accidental over-pressuring above the full scale and a large pressure reversal may be dangerous. Detailed studies of the metrological characteristics of CDGs and recommended practices for their calibration and use are given in [Hyland and Tilford 1985, Hyland and Shaffer 1991].

CDGs have to be calibrated. Even at low pressures, a linear behaviour cannot be assumed without verification, in particular since the conversion of the capacitance-bridge signal into a dc voltage output often includes a linearization. The calibration can be done (at various line pressures) using two pressure balances (a twin pressure balance facility is described

in [Fitzgerald *et al.* 2011]), or one pressure balance and a temperature-controlled reference volume, or even with a temperature-controlled (or monitored) vapour-pressure bath itself as the reference. In [Engert *et al.* 2007], the calibration was performed using a primary standard based on the static expansion method. By a special handling of the CDGs, a long-term stability within 0.02% over three years could be achieved. This is comparable with the stability of other high-accuracy low-pressure transducers [Miiller 1999]. Often CDGs are the transducers of choice because of their superior pressure resolution and all-metal construction.

In the null mode, temperature and line-pressure dependence, hysteresis, and stability of the zero are the limiting factors. High linearity is desirable for ease of calibration but is not essential. In this mode, the resolution may approach 1ppm of 100kPa and the temperature coefficient of the zero about $1\text{Pa} \cdot \text{K}^{-1}$. Repeatability is improved by pre-stressing the diaphragm in a given direction at a pressure corresponding to full scale deflection and taking care that afterwards the pressure never exceeds this value nor changes sign.

As a null instrument, the CDG has found wide application in gas thermometry, where it is used primarily to isolate the gas bulb from the manometer system. This allows a large reduction of the dead space and its associated errors, and also a greater flexibility in the application of pressure-measuring systems. For example, a pressure balance can be employed despite its inevitable gas leak [Berry 1979]. Using the CDG to measure residual pressure differences between the bulb and the pressure balance, rather than merely as a null instrument, compensates to some extent for the drawback that the balance can be operated only at discrete pressures.

In its absolute mode of operation (i.e. at zero backing pressure), the CDG can fill the gap left by the conventional pressure balance below 2kPa, where it offers a high enough accuracy for low-temperature thermometry, such as the realization of the ^3He vapour-pressure scale below 1K, see [Engert *et al.* 2007]. Finally, whenever the purity of a gas being used for thermometric purposes is a matter of concern, which is usually the case, it is worthwhile considering the use of an isolating CDG.

4.2. Thermomolecular pressure difference

A thermomolecular pressure difference (TMPD), also called thermal transpiration, will result from a temperature change along the pressure sensing tube if the diameter of the tube is not very large compared with the mean free path of the gas particles. The pressure at the higher-temperature end (frequently at room temperature) will be greater than the cryogenic bulb pressure due to this effect. The magnitude of this pressure difference depends on (i) the temperatures at both ends of the tube, (ii) the gas properties, (iii) the absolute pressure value, and thus (iv) the existing flow regime (viscous, intermediate, Knudson), (v) the tube diameter, (vi) the material of the tube, and (vii) the state of its internal surface, where (vi) and (vii) determine the accommodation coefficient.

A detailed overview of the existing empirical and theoretical models for describing the TMPD is given in [Pavese and Molinar Min Beciet 2013]. Unfortunately, it is concluded that a straightforward and elementary discussion of the effects does not exist. A widely used model equation has been developed starting with Weber and Schmidt (1936), generalised by McConville (1972), and approximated by Swenson (1989):

$$\frac{p_h - p_l}{p_l} = 2 \times 10^{-9} \left(\frac{r p_l}{\text{m} \times \text{Pa}} \right)^{-1.99} \left[(T_h / (\text{K}))^{2.27} - (T_l / (\text{K}))^{2.27} \right] \quad (4)$$

where p_h , p_l , T_h and T_l refer to the pressures and temperatures at the high and low temperature extremities, respectively, of a tube of diameter r .

Though it is recommended to apply Equation (4) for correcting for the TMPD in vapour-pressure thermometry, it should be considered that relative differences between calculations and experimental results are typically of the order of 20%. Lower uncertainties can be achieved only by performing in-situ investigations.

For the case of ^3He and ^4He vapour-pressure measurements, for a tube of constant diameter, more than 90% of the TMPD occurs between liquid nitrogen and room temperature. The magnitude of the effect can, therefore, be considerably reduced by employing a tube with two or more sections increasing in diameter from cold to hot [Sydoriak *et al.* 1964]. However, in the extreme case of ^3He vapour-pressure measurements at 0.65K, this requires extreme diameters as used in [Engert *et al.* 2007]. At this temperature, a uniform diameter of 5mm would still necessitate a correction of about 1mK temperature equivalent, with an uncertainty of at least 0.2mK without in-situ investigations.

5. UNCERTAINTY OF THE SCALE REALIZATION

The state-of-the-art level of accuracy of the realization of the helium vapour-pressure scales is represented by the uncertainty budgets established in [Engert *et al.* 2007], see Table 2. Since at higher temperatures, the magnitude of the estimates is of the same order, it can be stated that a realization of the vapour-pressure scales with standard uncertainties of order 0.2mK can be achieved applying modern high-purity gases and state-of-the-art techniques. This statement is mostly supported by the comparison between the realization of the ^3He vapour-pressure scale in [Engert *et al.* 2007] and the most recent data available in the literature [El Samahy 1979, Meyer and Reilly 1996, de Groot *et al.* 1993 and 1997] made in [Engert and Fellmuth 2003]. The comparison revealed only unresolved discrepancies of order 0.5mK below 1K with the data published in [Meyer and Reilly 1996].

References

- [1] Alasia F., Birello G., Capelli A., Cignolo G., Sardi M. 1999a The HG5 laser interferometer mercury manometer of the IMGC, *Metrologia* **36**, 499-503
- [2] Alasia F., Capelli A., Cignolo G., Gorla R., Sardi M. 1999b The MM1 laser interferometer low-range mercury manometer of the IMGC, *Metrologia* **36**, 505-509
- [3] Ambler E., Hudson R.P. 1956 An Examination of the Helium Vapor-Pressure Scale of Temperature Using a Magnetic Thermometer, *J. Res. Natl. Bur. Stand.* **56**, 99-104
- [4] Berry K.H. 1979 NPL-75: A Low Temperature Gas Thermometry Scale from 2.6K to 27.1K, *Metrologia* **15**, 89-115
- [5] Bock T., Ahrendt H., Jousten K. 2009 Reduction of the uncertainty of the PTB vacuum pressure scale by a new large area non-rotating piston gauge, *Metrologia* **46**, 389-396
- [6] Brombacher W.G., Johnson D.P., Cross J.L. 1960 *Mercury Barometers and Manometers*, NBS Monograph **8** pp.1-59
- [7] Cataland G., Edlow M.H., Plumb H.H. 1962 Recent Experiments on Liquid Helium Vapor Pressure Measurements from 2°K to 4°K, *Proc. Temperature: Its Measurement and Control in Science and Industry*, Vol. 3, Ed. F.G. Brickwedde (Reinhold Publishing Corporation, New York)pp. 413-417
- [8] Cawood W., Patterson H.S. 1933 The Capillary Depression of Mercury in Cylindrical Tubes and Some Errors of Glass Manometers, *Trans. Far. Soc.* **29**, 514-523
- [9] CIPM 1982 *Procès verbaux des séances* **8** and **T5-6**
- [10] Consultative Committee for Thermometry (CCT) 2010 Estimates of the Differences between Thermodynamic Temperature and the ITS-90, http://www.bipm.org/utls/common/pdf/ITS-90/Estimates_Differences_T-T90_2010.pdf
- [11] Dadson R.S., Lewis S.L., Peggs G.N. 1982 *The Pressure Balance. Theory and Practice* (Her Majesty's Stationary Office, London)
- [12] De Groot M.J., Mooikbroek J., Bloembergen P., Durieux M., Reesink A.L., Yuzhu M. 1993 International comparison of rhodium-iron resistance thermometers between 0,65K and 27K and measurement of helium vapour pressures, *Proc. 5th International Symposium on Temperature and Thermal Measurement in Industry and Science* (TEMPMEKO '93), 10-12November 1993 Prague, pp. 90-96
- [13] De Groot M.J., Gibb K., Heimeriks H. and Durieux M. 1997 The Measurement Of The Helium Vapour Pressure Between 0.53K and 1K, *Proc. International Seminar on Low Temperature Thermometry and Dynamic Temperature Measurement*, Ed. A. Szymrka-Grzebyk (DRUK, Wrocław) pp. L104-L109
- [14] Delajoud P., Girard M. 2002 A force balanced piston gauge for very low gauge and absolute pressure, *Proc. NCLSI Workshop and Symposium* (San Diego, CA, USA)

- [15] Durieux M., Astrov D.N., Kemp W.R.G., Swenson C.A. 1979, The Derivation and Development of the 1976 Provisional 0.5K to 30K Temperature Scale, *Metrologia* **15**, 57-63
- [16] Durieux M., Rusby R.L. 1983 Helium Vapour Pressure Equations on the EPT-76, *Metrologia* **19**, 67-72 El Samahy A E 1979 Thermometry between 0.5K and 30K, *Thesis* University of Leiden
- [17] Engert J., Fellmuth B. 2003 ^3He Vapour-Pressure Measurements at PTB, *Proc. Temperature: Its Measurement and Control in Science and Industry*, Vol. 7, Ed. D.C. Ripple *et al.* (AIP, Melville, New York) pp. 113-118
- [18] Engert J., Fellmuth B., Jousten K. 2007 A new ^3He vapour-pressure based temperature scale from 0.65K to 3.2K consistent with the PLTS-2000, *Metrologia* **44**, 40-52
- [19] Fellmuth B., Wolber L., Hermier Y., Pavese F., Steur P.P.M., Peroni I., Szmyrka-Grzebyk A., Lipinski L., Tew W.L., Nakano T., Sakurai H., Tamura O., Head D., Hill K.D., Steele A.G. 2005 Isotopic and other influences on the realization of the triple point of hydrogen, *Metrologia* **42**, 171-193
- [20] Fellmuth B., Fischer J., Machin G., Picard S., Steur P.P.M., Tamura O., White D.R., Yoon H. 2016 The kelvin redefinition and its *mise en pratique*, *Phil. Trans. R. Soc. A* **374**, 20150037, <http://rsta.royalsocietypublishing.org/content/roypta/374/2064/20150037>, DOI: 10.1098/rsta.2015.0037, Published 22 February 2016
- [21] Fitzgerald M., Sutton C., Jack D. 2011 New MSL twin pressure balance facility, *PTB-Mitt.* **121**, 263-265
- [22] Gould F.A., Vickers T. 1952 Capillary Depression in Mercury Barometers and Manometers *J. Sci. Instrum.* **29**, 85-87
- [23] Haines R., Bair M. 2002 Application of a wide method for the automated calibration of very low gauge and absolute pressures in a commercial calibration laboratory, presented at *2002 JAN Measurement Science Conference* (Anaheim, CA, USA)
- [24] Haines R., Bair M. 2009 A method of traceability for a FPG8601 force balanced piston gauge to define pressures in the range 1Pa to 15kPa in gauge and absolute measurement modes, *Proc. XIX IMEKO World Congress* (Lisbon, Portugal) pp. 2071-2076
- [25] Hendricks J.H., Olsen D.A. 2009 NIST experience with non-rotating force-balanced piston gauges for low pressure metrology, *Proc. XIX IMEKO World Congress* (Lisbon, Portugal) pp. 2077-2083
- [26] Hill K.D. 2002 Realizing the ITS-90 below 4.2K at the National Research Council of Canada, *Metrologia* **39**, 41-49
- [27] Hill K.D., Steele A.G. 2003 The Non-Uniqueness of the ITS-90: 13.8033K to 273.16K, *Proc. Temperature: Its Measurement and Control in Science and Industry*, Vol. 7, Ed. D.C. Ripple *et al.* (AIP, Melville, New York) pp. 53-58
- [28] Hyland R.W., Tilford C.R. 1985 Zero stability and calibration results for a group of capacitance diaphragm gages, *J. Vac. Sci. Technol.* **A3**, 1731-1737

- [29] Hyland R.W., Shaffer R.L. 1991 Recommended practices for the calibration and use of capacitance diaphragm gages as transfer standards, *J. Vac. Sci. Technol.* **A9**, 2843-2863
- [30] Kistemaker J. 1944-46 The Capillary Depression of Mercury and Precision Manometry, *Physica* **11**, 277-286
- [31] McConville G.T. 1972 The Effect of Measuring Tube Surface on Thermomolecular Corrections in Vapour Pressure Thermometry, *Proc. Temperature: Its Measurement and Control in Science and Industry*, Vol. 4, Ed. H.H. Plumb *et al.* (Instrument Society of America, Pittsburgh)pp. 159-169
- [32] Meyer C., Reilly M. 1996 Realization of the ITS-90 at the NIST in the range 0.65K to 5.0K using ^3He and ^4He vapour-pressure thermometry, *Metrologia* **33**, 383-389
- [33] Miiller A.P. 1999 Measurement performance of high-accuracy low-pressure transducers, *Metrologia* **36**, 617-621
- [34] Miiller A.P., Bergoglio M., Bignell N., Fen K.M.K., Hong S.S., Jousten K., Mohan P., Redgrave F.J., Sardi M. 2002 Final Report on Key Comparison CCM.P-K4 in Absolute Pressure from 1Pa to 1000Pa, *Metrologia* **39**, 07001
- [35] Nakano T., Tamura O., Sakurai H. 2007 Realization of Low-Temperature Fixed Points of the ITS-90 at NMIJ/AIST, *Int. J. Thermophys.* **28**, 1893-1903
- [36] Ooiwa A. 1989 Development of a highly stable air piston pressure gage with non-rotational piston-cylinder system, In: *High pressure metrology*, Ed. G. Molinar, *BIPM Monograph* 89/1 (Bureau International des Poids et Mesures, Sèvres), pp. 67-72
- [37] Ooiwa A. 1993/1994 Novel Nonrotational Piston Gauge with Weight Balance Mechanism for the Measurement of Small Differential Pressures, *Metrologia* **30**, 607-610
- [38] Otal P., Legras J.C. 2005 Metrological characterisation of a new standard, in absolute and gauge pressure modes, in the range 1Pa to 15 000Pa, *Metrologia* **42**, S216-S219
- [39] Pavese F., Steur P.P.M., Jin Seog Kim, Giraudi D. 2011 Further results on the triple point temperature of pure ^{20}Ne and ^{22}Ne , *J. Chem. Thermodyn.* **43**, 1977-1983
- [40] Pavese F., Molinar Min Beciet G. 2013 *Modern Gas-Based Temperature and Pressure Measurements* (Springer Science + Business Media, New York)
- [41] Pokhodun A.I., Fellmuth B., Pearce J.V., Rusby R.L., Steur P.P.M., Tamura O., Tew W.L., White D.R. 2016 Platinum Resistance Thermometry, *Guide to the realization of the ITS-90*:Chapter 5, <http://www.bipm.org/utls/common/pdf/ITS-90/Guide-ITS-90-Platinum-Resistance-Thermometry.pdf>
- [42] Preston-Thomas H. 1990 The International Temperature Scale of 1990 (ITS-90), *Metrologia* **27**, 3-10, 107
- [43] Pirruenrom T. 2011 *Development of Pressure Balances for Absolute Pressure Measurement in Gases up to 7MPa* (Papierflieger-Verlag, Clausthal-Zellerfeld), ISBN 978-3-86948-178-4

- [44] Quinn T.J. 1990 *Temperature* (Academic Press Limited, London)
- [45] Rendle C.G. 1993/1994 A Large Area Piston Gauge for Differential and Gauge Pressure from Zero to 3, 2kPa, *Metrologia* **30**, 611-613
- [46] Rendle C.G., Rosenberg H. 1999 New absolute pressure standard in the range 1Pa to 7kPa, *Metrologia* **36**, 613-615
- [47] Rusby R.L., Durieux M. 1984 Inverted forms of the new helium vapour pressure equations, *Cryogenics* **24**, 363-366
- [48] Rusby R.L., Swenson C.A. 1980 A New Determination of the Helium Vapour Pressure Scales Using a CMN Magnetic Thermometer and the NPL-75 Gas Thermometer Scale, *Metrologia* **16**, 73-87
- [49] Sabuga W. 2011a Pressure measurements in gas media up to 7.5MPa for the Boltzmann constant redetermination, *PTB-Mitt.* **121**, 247-255
- [50] Sabuga W., Sharipov F., Priuenrom T. 2011b Determination of the Effective Area of Piston-Cylinder Assemblies Using a Rarefied Gas Flow Model, *PTB-Mitt.* **121**, 260-262
- [51] Sadkovskaja I., Eichwald A. 2011 The laser interferometric oil manometer with floats, *PTB-Mitt.* **121**, 301-302
- [52] Sakurai H. 2003 Calorimetric study of the triple point of equilibrium hydrogen, *Proc. 8th International Symposium on Temperature and Thermal Measurements in Industry and Science* (TEMPMEKO 2001), Ed. B. Fellmuth, J. Seidel, G. Scholz (VDE Verlag GmbH / Berlin) ISBN 3-8007-2676-9, pp. 411-416
- [53] Shimazaki T., Toyoda K., Tamura O. 2011 Realization of the ^3He Vapor-Pressure Temperature Scale and Development of a Liquid-He-Free Calibration Apparatus, *Int. J. Thermophys.* **32**, 2171-2182
- [54] Sommer K.D., Poziemski J. 1993/1994 Density, thermal expansion and compressibility of mercury, *Metrologia* **30**, 665-668
- [55] Sparasci F., Pitre L., Rouillé G., Thermeau J.-P., Truong D., Galet F., Hermier Y. 2011a An Adiabatic Calorimeter for the Realization of the ITS-90 in the Cryogenic Range at the LNE-CNAM, *Int. J. Thermophys.* **32**, 201-214
- [56] Sparasci F., Pitre L., Truong D., Risegari L., Hermier Y. 2011b Realization of a ^3He – ^4He Vapor-Pressure Thermometer for Temperatures Between 0.65K and 5K at LNE-CNAM, *Int. J. Thermophys.* **32**, 139-152
- [57] Steur P.P.M., Fellmuth B., Tamura O. 2015 Interpolating Constant-Volume Gas Thermometry, *Guide to the realization of the ITS-90*: Chapter 4, <http://www.bipm.org/utls/common/pdf/ITS-90/Guide-ITS-90-GasThermometry-2015.pdf>
- [58] Steele A.G. 1997 Fixed-point cryostat using closed-cycle refrigerator: Design and control, *Proc. International Seminar on Low Temperature Thermometry and Dynamic Temperature Measurement*, Ed. A. Szmyrka-Grzebyk (DRUK, Wrocław) pp. L48-L53

-
- [59] Sullivan J.J. 1985 Development of variable capacitance pressure transducers for vacuum applications, *J. Vac. Sci. Technol.* **A3**, 1721-1730
- [60] Sutton C.M., Fitzgerald M.P. 2009 Performance aspects of gas-operated pressure balances as pressure standards, *Metrologia* **46** 655-660
- [61] Swenson C.A. 1989 Supplementary Information for ITS-90 – Interpolating gas thermometer, Comité Consultatif de Thermométrie, 17^e Session, Doc. CCT/89-27
- [62] Sydoriak S.G., Sherman R.H., Roberts T.R. 1964 The 1962 He³ Scale of Temperature. Parts I to IV, *J. Res. Natl. Bur. Stand.* **68A**, 547-588
- [63] Tilford C.T. 1993/1994 Three and a Half Centuries Later – The Modern Art of Liquid-column Manometry, *Metrologia* **30**, 545-552
- [64] Weber S., Schmidt G. 1936 Experimentelle Untersuchungen über die thermomolekulare Druckdifferenz in der Nähe der Grenzbedingung $p_1/p_2 = \sqrt{(T_1/T_2)}$ und Vergleichung mit der Theorie *Leiden Commun.* **246C** 1-13
- [65] Yang I., Song C.H., Kim Y.-G., Gam K.S. 2011 Cryostat for Fixed-Point Calibration of Capsule-Type SPRTs, *Int. J. Thermophys.* **32**, 2351-2359
- [66] Zandt T., Sabuga W., Gaiser C., Fellmuth B. 2015 Measurement of pressures up to 7MPa applying pressure balances for dielectric-constant gas thermometry, *Metrologia* **52** 305-313